

Original Article

Inhibition of CDK2 reduces EZH2 phosphorylation and reactivates ER α expression in high-grade serous ovarian carcinoma

Ye Han^{1,2}, Yongkun Wei², Jun Yao², Yu-Yi Chu², Chia-Wei Li², Jennifer L Hsu², Lei Nie², Mien-Chie Hung^{3,2}

¹The Second Breast Surgery Section, Shengjing Hospital of China Medical University, Shenyang, P. R. China;

²Department of Molecular and Cellular Oncology, The University of Texas MD Anderson Cancer Center, Houston, Texas, USA; ³Graduate Institute of Biomedical Sciences, Research Center for Cancer Biology, and Center for Molecular Medicine, China Medical University, Taichung 404, Taiwan

Received February 14, 2020; Accepted March 20, 2020; Epub April 1, 2020; Published April 15, 2020

Abstract: The cyclin-dependent kinase 2 (CDK2) inhibitor dinaciclib, a potential anti-cancer drug, has been tested in clinical trials and reported to suppress tumor initiating cells. Our recent study demonstrated that pharmacological inhibition of CDK2 or enhancer of zeste homolog 2 (EZH2) allows re-expression of ER α and converts triple-negative breast cancers (TNBC) to luminal ER α -positive, rendering TNBC cells targetable by tamoxifen. Like TNBC, EZH2 is also commonly overexpressed in ovarian cancers, and overexpression of cyclin E1 gene (CCNE1) and/or amplification of its associated kinase *CDK2* gene is present in ovarian tumor specimens, both of which are associated with primary treatment resistance and poor outcome in high-grade serous ovarian cancer (HGSC). We determined whether inhibition of CDK2-mediated phosphorylation of EZH2 activates ER α expression in ER α -negative HGSOC cells, rendering them targetable by hormonal therapy. The specific CDK2 inhibitor repressed phosphorylation of EZH2 at T416, and in turn activated the expression of its downstream target ER α gene (*ESR1*). We tested the efficacy of the combination of CDK2 inhibitor and tamoxifen and found significant synergistic inhibition. We further demonstrated that CDK2 inhibitor is a more promising agent than EZH2 inhibitor in repressing TNBC and HGSOC due to a feedback increase in CDK2 activity by EZH2 inhibitor. Our results indicated that the combination treatment of CDK2 inhibitor and tamoxifen has the potential to benefit patients with ER α -negative HGSOC.

Keywords: EZH2, CDK2, ER α , HGSOC, phosphorylation

Introduction

EZH2 is the core component of the PRC2 complex and catalyzes H3K27 trimethylation to silence its target genes [1-4]. Studies have shown that EZH2 is one of the key epigenetic factors involved in maintaining self-renewal, pluripotency, and differentiation of embryonic and adult stem cells [2-6]. We previously showed that expression of EZH2 sustains a reversible and undifferentiated stem cell-like phenotype in breast cancer cells and contributes to their expansion [6-8]. It has also been reported that elevated expression of EZH2 correlates with poorly differentiated breast carcinomas and poor prognosis in many types of solid tumors [9]. Thus, EZH2 may serve as a therapeutic target whose inactivation de-repre-

sents its downstream genes [9, 10]. Tazemetostat (EPZ-6348), a highly selective EZH2 inhibitor, is currently under evaluation in clinical trials for different types of cancers and has been submitted for FDA approval in July 2019. The FDA granted priority review to tazemetostat for the treatment of patients with metastatic or locally advanced epithelioid sarcoma who are not eligible for curative surgery and has been first approved in January 23, 2020.

Ovarian cancer is the second most lethal gynecological malignancy with the highest mortality rate and relapses in about 70% patients after primary surgery and chemotherapy [11-14]. High-grade serous ovarian carcinoma (HGSOC) is the most frequent type (> 70% of epithelial ovarian cancer) of ovarian cancers and acc-

CDK2 inhibitor inhibits phosphorylation of EZH2 to activate ER α expression

counts for the most tumor-associated mortalities [15, 16]. The *CCNE* gene, which encodes cyclin E, is one of the most frequently amplified genes in HGSOC [17]. Cyclin E mainly coordinates with cyclin-dependent kinase 2 (CDK2) to facilitate G1/S cell cycle progression. In ovarian cancers, elevated *CCNE1* is often correlated with higher CDK2 expression, and most of *CCNE1*-associated tumor promoting effects require the participation of CDK2 [18]. Therefore, CDK2 is a feasible target in HGSOC patients with high CDK2 expression. Currently, CDK2 inhibitor dinaciclib is under investigation in a phase 2/3 clinical trial, and preliminary results showed encouraging single-agent activity in patients with relapsed multiple myeloma [19]. In randomized phase II clinical trial for the patients with advanced breast cancer, dinaciclib monotherapy demonstrated some antitumor activity and was generally tolerated although the efficacy was not superior to capecitabine chemotherapy [20, 21]. Thus, it is worthwhile to evaluate dinaciclib in selected patient populations with metastatic breast cancer and in combination with other agents. HGSOC is a highly heterogeneous disease with extremely poor prognosis and limited therapeutic options [11, 16]. Because the ovaries are hormonal related organs and most HGSOCs are highly invasive, the development of novel therapeutic strategies remains an obstacle to overcome [11, 16, 22], which encouraged us to develop an effective combination therapy for this highly invasive cancer.

The female sex hormone estrogen is mainly secreted by the ovaries and originated in granulosa cells. The ovarian surface epithelium is the main cell type of the ovaries. In epithelial ovarian cancers, the estrogen receptor (ER)-positive rate is about 43-81%, depending on the methodological criteria [11, 15, 22, 23]. ER α belongs to members of the steroid receptor superfamily and plays a crucial physiological roles of the target organs, including genital tract, bone, mammary glands, adipose tissues, and brain, as transcriptional factors [24]. A large number of ovarian tumor tissue microarray analyses indicated that ER α expression is high in 60.2% and low or negative in 20.5% of HGSOC (n = 1691, The Cancer Genome Atlas) [11, 25], which is similar to that (81%) in breast cancer, a disease which has been treated by hormone therapy for decades [26]. However, about 20-

30% of patients with HGSOC who are ER α -negative show poor response to hormone therapy [27].

Tamoxifen (TAM) is not the first non-steroidal anti-estrogen treatment but has been widely used to treat women with luminal breast cancer before menopause [28]. TAM binds to ER instead of estrogen to block ER α signaling [29]. In a recent study, we demonstrated that CDK2 and EZH2 inhibitors can induce ER α re-expression in TNBC and that the combination therapy of CDK2 or EZH2 inhibitor and TAM may be a promising approach for TNBC [30]. Clinical studies indicated that patients with relapsed HGSOC and an ER histoscore > 200 who received endocrine therapies have significant greater benefits [31]. They also showed that the degree of ER expression is proportional to endocrine sensitivity in HGSOC [31]. The similarity in limited treatment options and poor prognosis between ER α -negative HGSOC and TNBC led us to determine whether blockade of the CDK2/EZH2 axis converts ER α negative to positive and renders HGSOC targetable by hormone therapy.

Methods

Cell line cultures and reagents

All cell lines were obtained from the ATCC (Manassas, VA) and independently validated by STR DNA fingerprinting at The University of Texas MD Anderson Cancer Center, and tests for mycoplasma contamination were negative. TNBC cell lines BT-549 and MDA-MB-231, and ovarian cancer cell lines SKOV3, OVCA433, CAOV3, DOV13, A2780, OVCA420 were cultured in DMEM (Hyclone) supplemented with 10% FBS and penicillin and streptomycin. All cells were incubated at 37°C with 5% CO₂. EPZ-6438, 3-deazaneplanocin A hydrochloride, dinaciclib, and GSK343 were obtained from Selleckchem (Houston, TX). Antibodies against EZH2 and phospho-CDK2 were obtained from Cell Signaling (Danvers, MA). Antibodies against ER α (ab108398) was purchased from Abcam (Cambridge, MA).

Bioinformatics analysis

For genetic alternation analysis of *EZH2* gene, the cbiportal (<http://www.cbiportal.org>) was queried for 'EZH2', and the frequency of altera-

CDK2 inhibitor inhibits phosphorylation of EZH2 to activate ER α expression

tion of *EZH2* in related tumors is shown as a bar graph. To identify TCGA ovarian tumors with *EZH2* gene overexpression (OE), we used data from normal ovarian tissue in TCGA and Yoshihara [32], and set up a cutoff at two standard deviation (SD) above median normal expression of *EZH2*. RNAseq dataset of Yoshihara includes a total 43 ovarian cancer samples and 10 normal ovarian tissues; TCGA includes a total 586 ovarian cancer samples and 8 normal tissues.

RNA extraction and real-time PCR

The HGSOC cells were treated with CDK2 inhibitor (CDK2i) or EZH2 inhibitor (EZH2i) for 3 days, and total RNA was extracted from the treated cell pellets with Trizol. The SuperScript III First Strand Synthesis System was used for RT-PCR (Invitrogen). Real-time PCR was performed using SYBR Green-base PCR (Qiagen). The primer sequences for the transcripts analyzed are as follows (5' to 3'):

<i>ESR1</i>	FORWARD	CTCTCCACATCAGGCACA
	REVERSE	CTTTGGTCCGTCTCCTCCA
<i>GAPDH</i>	FORWARD	GAAGGTGAAGGTCGGAGTC
	REVERSE	GAAGATGGTGATGGGATTTTC
<i>PGR</i>	FORWARD	CTTAATCAACTAGGCGAGAG
	REVERSE	AAGCTCATCCAAGAATACTG
<i>TFF1</i>	FORWARD	GTCCCTGGTGCTTCTATCC
	REVERSE	GAGTAGTCAAAGTCAGAGCAGTCAATCT
<i>c-MYC</i>	FORWARD	GAAGATGGTGATGGGATTTTC
	REVERSE	GAAGATGGTGATGGGATTTTC

Immunoblotting analysis

Whole-cell extracts were lysed in radioimmunoprecipitation buffer (RIPA, 10 mM Tris-HCl [pH 8.6], 1 mM EDTA, 1% Triton X-100, 0.1% sodium deoxycholate, 0.1% sodium dodecyl sulfate (SDS), 140 mM NaCl, and 1 \times protease inhibitor; Complete Mini, Roche), which was freshly added before lysis. Total protein extracts (20–30 μ g) from each sample were separated on 10% polyacrylamide gel and transferred onto a polyvinylidene difluoride membrane (Life Technologies). Antibodies against ER α , H2K27Me3, and phospho-CDK2 were incubated with the membranes overnight at 4 $^{\circ}$ C after blocking in 5% non-fat milk for one hour followed by secondary anti-mouse-HRP or anti-rabbit-HRP (Cell Signaling) at room temperature for 1 hour. The membranes were washed with PBS-Triton buffer and imaged using ECL reagents (Bio-Rad Laboratories) in ImageQuant LAS 4010 (GE Healthcare).

MTT assay and calculation of combination index (CI) of drug synergy

For the MTT assay, SKOV3 (3,000 cells per well), OVCA433 (5,000 cells per well), and CAOV3 (4,000 cells per well) were seeded in a 96-well plate and cultured overnight before treatment. Cells were then treated with inhibitors either alone or in combination at the indicated concentrations for 3 days. MTT reagent was added into each well at a final concentration of 0.5 μ g/ml and incubated for 30 min before formazan was extracted with DMSO. Cell survival was calculated using an absorbance at 590 nm and normalized to that of the untreated wells. The half maximal inhibitory concentration (IC_{50}) was calculated using MTT data and GraphPad Prism 8.0. Chou-Talalay combination index (CI) were calculated by using Compusyn software (www.combosyn.com) with cell survival data from the MTT assay. Drug combinations were designed using the constant ratio of 2 inhibitors according to the predictions by the Compusyn program [33, 34]. Criteria for CI: $CI \leq 0.3$, strong synergy; $0.3 < CI \leq 0.85$, synergy.

Tumor-sphere formation assay in 3D matrigel

Three-dimensional (3D) culture was performed as previously described [6, 30]. Briefly, pre-chilled culture 24-well plates were coated with a thin layer of cold growth factor-reduced Engelbreth-Holm-Swarm extracellular matrix extract (EHS; Matrigel, BD Biosciences, San Jose, CA). The plates were then incubated for 30 min at 37 $^{\circ}$ C to allow EHS gelation. MDA-MB-231 (5,000) cells were suspended in the culture medium containing 2.5% Matrigel, seeded on Matrigel-coated 24-well plate, and incubated at 37 $^{\circ}$ C for 3 days followed by treatment with CDK2 and/or EZH2 inhibitor for 1 week. A representative area of MDA-MB-231 tumorsphere cultures was imaged. The number of spheres formed per field was quantified ($n = 10$).

Results

Previous studies showed that cyclin E/CDK2 phosphorylates EZH2 at T416 and activates EZH2 [6, 35]. Phosphorylation of EZH2 at T435 and T487 by CDK1 and CDK2 epigenetically silences target genes in breast cancers [5, 6, 36, 37]. Inhibition of CDK2 or EZH2 has been

CDK2 inhibitor inhibits phosphorylation of EZH2 to activate ER α expression

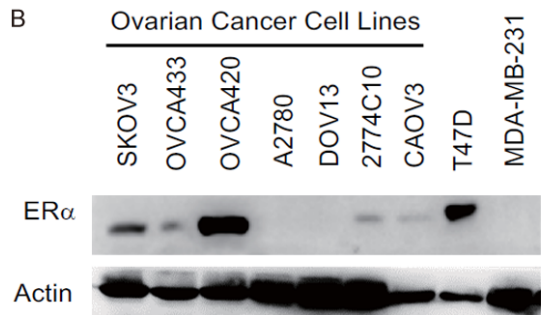
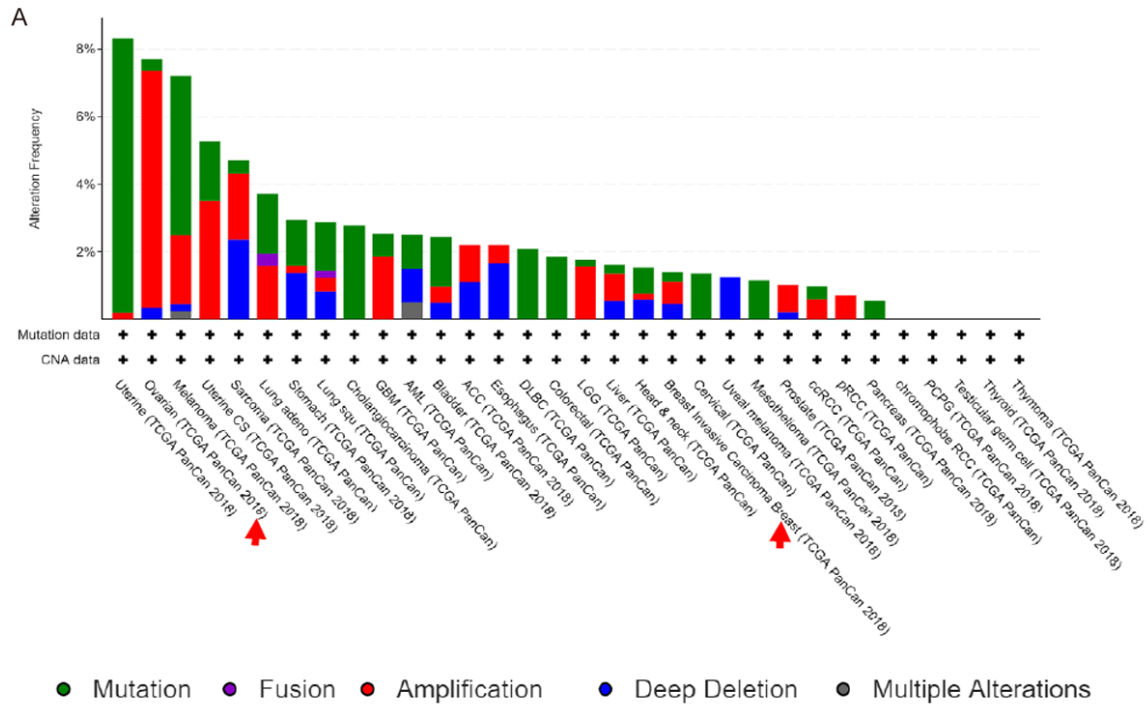


Figure 1. Expression of EZH2 in ovarian cancers. A. Alterations of EZH2 in human cancers. The alterations of 'EZH2' was queried using bioinformatics platform cBioportal (<http://www.cbioportal.org>). Bar graph showing the frequency of alteration of EZH2 in related tumors. Breast and ovarian cancers are highlighted with red arrows. B. The ER α proteins in the whole cell lysates of the ovarian cancer cell lines were immunoblotted with specific antibodies as indicated. T47D cell line was used as ER α positive and MDA-MB-231 cell line as ER α negative control.

found to reverse epigenetic silencing and induces downstream gene such as ER α re-expression in TNBC [30]. In the present study, we determined whether inhibition of the CDK2/EZH2 signaling pathway by specific inhibitors induces ER α expression in ovarian cancer cells and tested the efficacy of combination treatment of CDK2i or EZH2i and tamoxifen (TAM) in vitro. We also explored the putative feedback mechanism of CDK2 activity triggered by EZH2i in TNBC and HGSOC cells.

EZH2 and ER α expression in ovarian cancer cells

The classical ER α has been shown to originate from the ovarian surface epithelium although only a small number of ovarian cancers respond to anti-estrogen therapy [11, 16, 31]. A previous study showed that phosphorylation of

EZH2 by CDK2 initiates the epigenetic silencing of downstream target genes, leading to the repression of ER α expression in vitro and in vivo [30]. To expand our study to ovarian cancer, we first sorted out the EZH2 expression and mutation in various cancers according to TCGA and Yoshihara database [32]. At first, the cBioPortal platform (<http://www.cbioportal.org>) was used to query for gene alternations of 'EZH2'. Bar graph displayed the frequency of alteration of EZH2 in related tumors. EZH2 alternations including mutations, amplifications, deletions, fusions, and multiple mutations were found in many types of cancers (Figure 1A). The rate of frequency of EZH2 amplification (> 7%) in ovarian cancer was the highest among a panel of cancer types examined (Figure 1A, red arrows). To determine the expression levels of EZH2 in ovarian cancers, we analyzed two sets of RNAseq databases of

CDK2 inhibitor inhibits phosphorylation of EZH2 to activate ER α expression

Table 1. Overexpression (OE) of EZH2 in ovarian cancer

Dataset	Normal	Tumor	Media N	Media T	OE Normal	OE Tumor
Yoshihara [32]	10	43	0.912	3.496	0	86%
TCGA	8	586	-1.044	1.876	0	95%

TCGA and Yoshihara RNAseq Dataset; OE, overexpression; N, normal; T, tumor.

TCGA and Yoshihara [32], and the results revealed EZH2 is overexpressed in 95% and 86% of patients with ovarian cancer (**Table 1**). The lists of patient samples of ovarian cancers with EZH2 overexpression are provided in [Tables S1](#) and [S2](#). Because activation of the EZH2-containing PRC2 complex serves as an initiator for epigenetic silencing of ER α expression, we next examined the expression of ER α in HGSOC cells. We at first performed Western blot analysis to screen the available ovarian cancer cell lines and selected those with silenced ER α gene expression. As shown in **Figure 1B**, compared with luminal breast cancer cell line T47D and TNBC cell line MDA-MB-231, the ER α protein levels in five of the seven HGSOC cell lines (SKOV3, A2780, DOV13, 2774C10 and CAOV3) examined were low or undetectable. Thus, we used those five cell lines to further examine ER α expression in response to the treatment of CDK2i and EZH2i.

CDK2i reactivates ESR1 gene expression in ER α -negative ovarian cancer cell lines

The *ESR1* gene encoding ER α is one of the well-identified EZH2 target genes [30]. To determine whether blockade of the CDK2/EZH2 axis by CDK2i reactivates *ESR1* expression and thus renders cancer cells sensitive to TAM, we treated several ovarian cancer cell lines with CDK2i and performed quantitative real-time PCR assays to determine the mRNA levels of ER α . Because CDK2 is an upstream kinase that regulates EZH2 activity via site-specific phosphorylation at T416 [6, 35, 37], we treated ER α -low or -negative ovarian cancer cells with either CDK2i or EZH2i for 3 days followed by Western blot analysis of whole cell lysates. Among the ovarian cancer cell lines examined, only SKOV3, OVCA433 and CAOV3 re-expressed ER α in response to treatment with CDK2i dinaciclib (DINA; **Figure 2A**). Next, we examined the ER α and H3K27Me3 levels in CDK2i-sensitive HGSOC cells and showed that ER α was re-expressed with concomitant decrease in H3K27Me3 levels after treatment with CDK2i

and EZH2i (**Figure 2B**). To determine whether CDK2i-induced ER α occurs at the transcriptional or translational level and whether the induced ER α is functional, we compared the mRNA levels of *ESR1* and the well-defined ER α downstream target genes including *C-MYC*, *TFF1*, and *PGR*, in CDK2i-treated HGSOC cells by quantitative real-time PCR. The expression levels of ER α and its target genes were significantly increased after 3-day treatment with CDK2i (50 nM) and high concentration of EZH2i (GSK343, 10 μ M) (**Figure 2C-F**, $P < 0.05$ and 0.001). These results suggested that both CDK2 and EZH2 inhibitors block the CDK2/EZH2 axis to release the epigenetic repression of *ESR1*, which in turn upregulates the expression of its downstream target genes *PGR*, *TFF1*, and *C-MYC*. Blockade of the CDK2/EZH2 axis leads to reactivation of functional ER α , as indicated by upregulated ER α target genes *PGR*, *TFF1*, and *c-Myc*, and in turn renders ER α -negative HGSOC targetable by hormone therapy.

TAM in combination with CDK2i or EZH2i induces synergistic inhibitory effects on HGSOC

TAM has been the gold standard of hormone therapy for ER-positive breast cancer for almost 40 years and is also used to treat ovarian cancer. Previously, we reported that inhibition of EZH2 phosphorylation by CDK2i induces ER α re-expression in TNBC and that the combination of CDK2i or EZH2i and TAM synergistically reduces TNBC proliferation *in vitro* and *in vivo* [30]. Accordingly, we asked whether this strategy also applies to HGSOC with low or negative ER α expression. To this end, HGSOC cells were treated with either CDK2i (dinaciclib, DINA) or EZH2i (GSK343, GSK) combined with TAM at different concentration ratios. The drug interactions between CDK2i or EZH2i and TAM were determined by MTT assay. Similar to our observations in TNBC, the combination of either CDK2i or EZH2i with TAM also synergistically inhibited proliferation of the ovarian cancer cell lines tested *in vitro* (**Figure 3A-C**; CI val-

CDK2 inhibitor inhibits phosphorylation of EZH2 to activate ER α expression

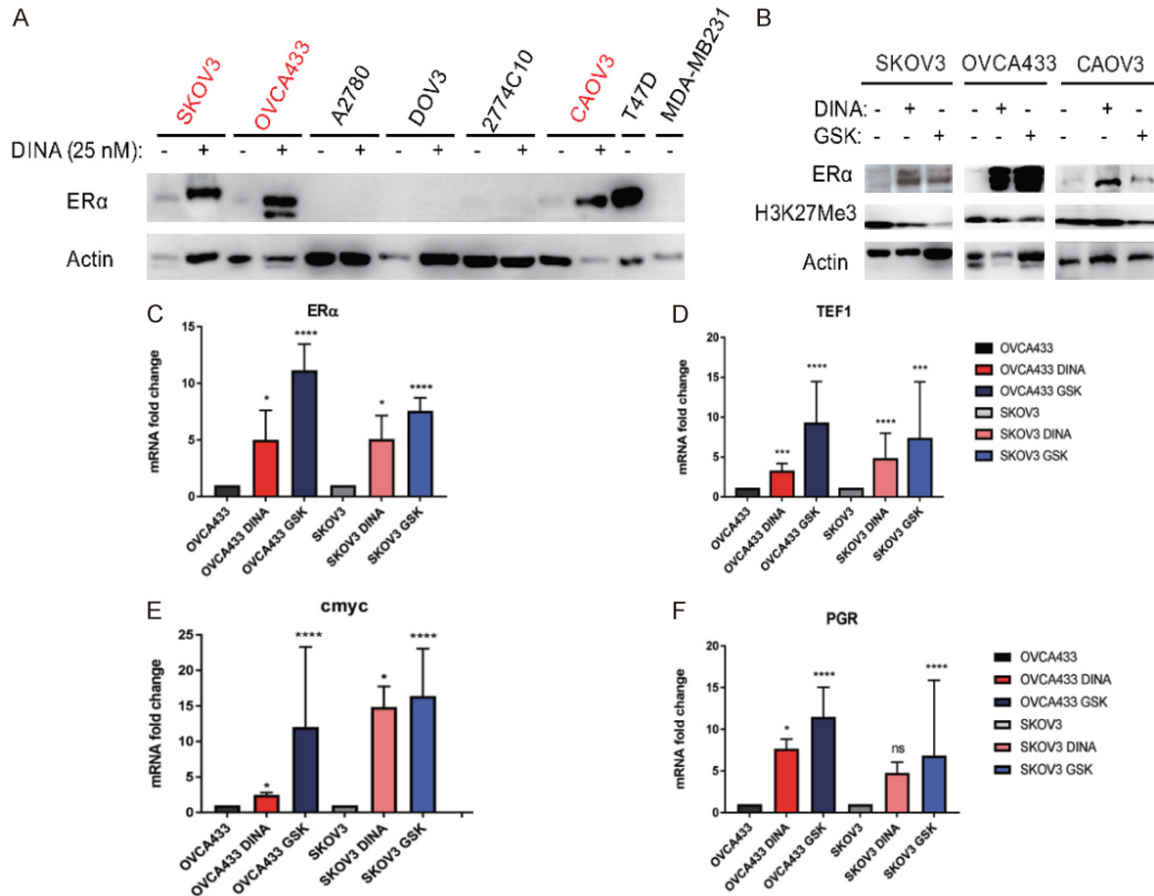


Figure 2. CDK2 inhibitor induces expression of ER α in ER α -negative ovarian cancer cell lines. A. Selected ER-negative ovarian cancer cell lines were treated with 25 nM dinaciclib (DINA) for 3 days. ER α , EZH2, and H3K27Me3 protein levels in whole cell lysates were detected by Western blot analysis with specific antibodies against ER α after treatment with CDK2i (DINA). B. Western blot analysis of ER α , EZH2, and H3K27Me3 in HGSOC cells after treatment with 25 nM (DINA) or 10 μ M GSK343 (GSK) for 72 hours. C-F. qPCR analyses of mRNA levels of ER α and its downstream target genes Pgr, TFF1, and c-Myc are shown as mean \pm SD (n = 3). *P < 0.05, ***P < 0.01, and ****P < 0.001, Student's t-test. ns, no significance.

ues < 0.8). Blockade of the EZH2/CDK2 axis with CDK2i or EZH2i reactivated ER α expression and sensitized HGSOC to hormone therapy, suggesting that this combination is effective in both TNBC and HGSOC.

Feedback regulation of the CDK2-EZH2 signaling axis in breast and ovarian cancers

CDK2 plays a crucial role in both cell cycle progression and apoptotic response, and cyclin E/CDK2 phosphorylates EZH2 at T416 [6, 35, 37]. We previously tested a CDK2 inhibitor, dinaciclib, and two EZH2 inhibitors, EPZ-6438 and GSK343, all of which have been evaluated in clinical trials and target different steps of the CDK2/EZH2 signaling axis. Interestingly, in pre-

vious study we found that the effectiveness and potency of these EZH2i and CDK2i inhibitors were different [30]. CDK2i inhibits EZH2 phosphorylation upstream of the CDK2-EZH2 axis and indirectly represses EZH2 activity [30]. In contrast, EZH2i directly binds to the SET domain, resulting in a decreased histone methyltransferase of EZH2 complex at the promoter of the target genes [38]. Accordingly, EZH2i should be more effective since it directly blocks the terminal regulator of the CDK2-EZH2 axis. To this end, ER α -negative cancer cells were treated with 5 μ M EPZ-6438, an already FDA-approved drug, GSK343, or CDK2i dinaciclib (50 nM) for 3 days. Immunoblot analyses of the drug- and vehicle-treated cancer cells revealed that CDK2i was more effective than EZH2i in

CDK2 inhibitor inhibits phosphorylation of EZH2 to activate ER α expression

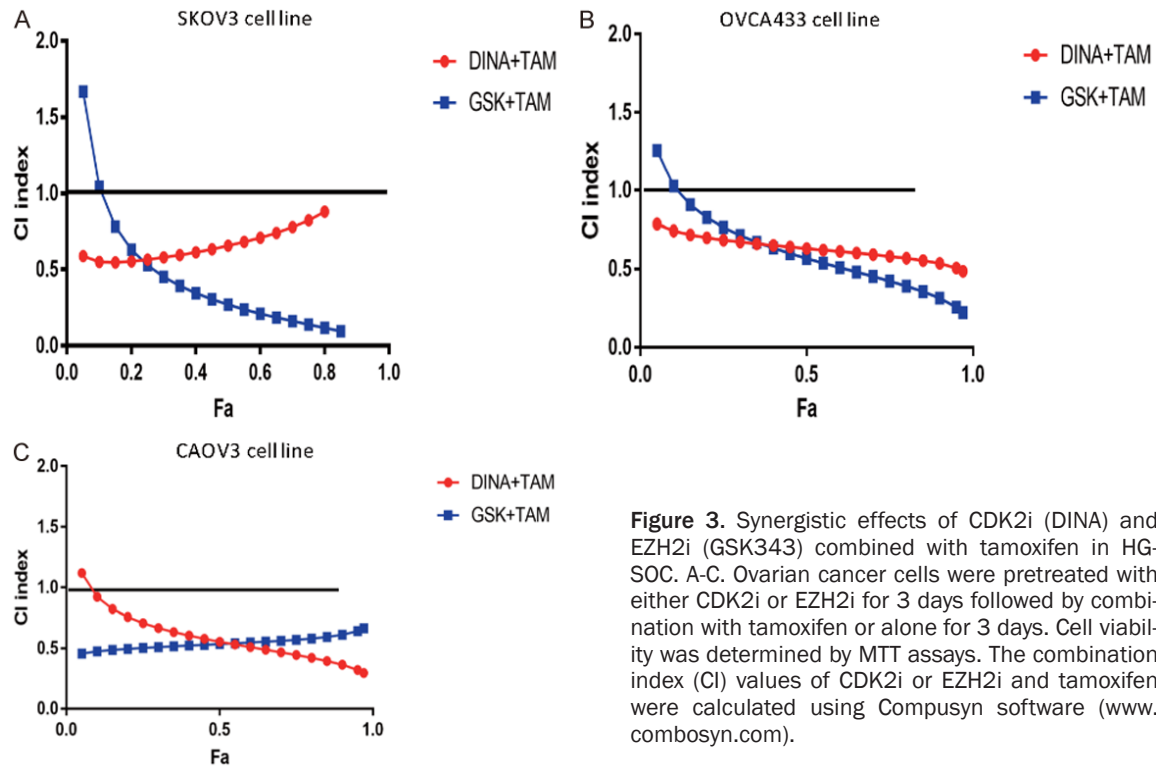


Figure 3. Synergistic effects of CDK2i (DINA) and EZH2i (GSK343) combined with tamoxifen in HG-SOC. A-C. Ovarian cancer cells were pretreated with either CDK2i or EZH2i for 3 days followed by combination with tamoxifen or alone for 3 days. Cell viability was determined by MTT assays. The combination index (CI) values of CDK2i or EZH2i and tamoxifen were calculated using Compusyn software (www.combosyn.com).

inducing ER α expression (**Figure 4A**, 50 nM dinacililb vs. 5 μ M GSK343). Notably, as shown in **Figure 4A**, treatment with 5 μ M EPZ-6438 did not activate ER α expression, suggesting that the efficacy of EPZ-6438 is not as potent as GSK343 in vitro. Additionally, treatment with 100 nM SNS032, a CDK2i that is also in clinical trial, significantly reactivated ER α expression in TNBC cells (**Figure 4B**). These observations are consistent with those reported in the previous studies [30]. Compared with GSK343, EPZ-6438 was less effective in ER α induction in vitro (**Figure 4A**, lane 2 vs lane 3). However, treatment with EPZ-6438 at higher concentrations (≥ 10 μ M) also induced ER α expression in TNBC cells (**Figure 4C**). Moreover, using tumor-sphere formation assay in 3D Matrigel culture, we examined the sensitivity of TNBC cells to the inhibitors. The results revealed that both EZH2i and CDK2i significantly reduced tumorsphere formation with CDK2i showing stronger inhibitory effect than did EZH2i in this functional assay (**Figure 4D** and **4E**). To validate that CDK2i-induced ER α is dependent on EZH2, we knocked down EZH2 in MDA-MB-231 cells using shRNA against EZH2 (sh-EZH2). Indeed, compared with control sh-RNA against luciferase (sh-Luc) cells, ER α expression was signifi-

cantly increased after depletion of EZH2 (**Figure 5A**, lanes 1 and 4). Intriguingly, CDK2i-induced ER α expression in sh-EZH2 cells was not significantly increased compared with that in sh-Luc control cells even with 100 nM of DINA (**Figure 5A**, lane 3 vs. 6; lane 4 vs. 6), suggesting that CDK2i-induced ER α expression is at least partially dependent on EZH2, and as a result, depletion of EZH2 attenuates CDK2-mediated reactivation of ER α expression. Next, we determined whether inhibition of EZH2 activity regulates CDK2 activity by a feedback mechanism in the signaling pathway. To this end, we tested the effects of three EZH2i, GSK343, 3-deazaneplanocin A hydrochloride (DZNEP), and EPZ-6438 on CDK2 activity in TNBC and HGSOC cell lines. MDA-MB-231 TNBC cells were treated with EZH2i for 72 hours, the ER α , EZH2 and pCDK2 protein levels in these cells were immunoblotted with specific antibody against activated CDK2, pCDK2(T160). EZH2i treatment significantly enhanced pCDK2 along with ER α expression in MDA-MB-231 cells compared with that in vehicle control and sh-EZH2 cells (**Figure 5B**, lanes 1 and 2). Notably, deletion of EZH2 significantly reduced pCDK2 (**Figure 5B**, lane 1 vs. 2), suggesting that EZH2 stabilizes pCDK2 in the CDK2/EZH2 complex. Similar

CDK2 inhibitor inhibits phosphorylation of EZH2 to activate ER α expression

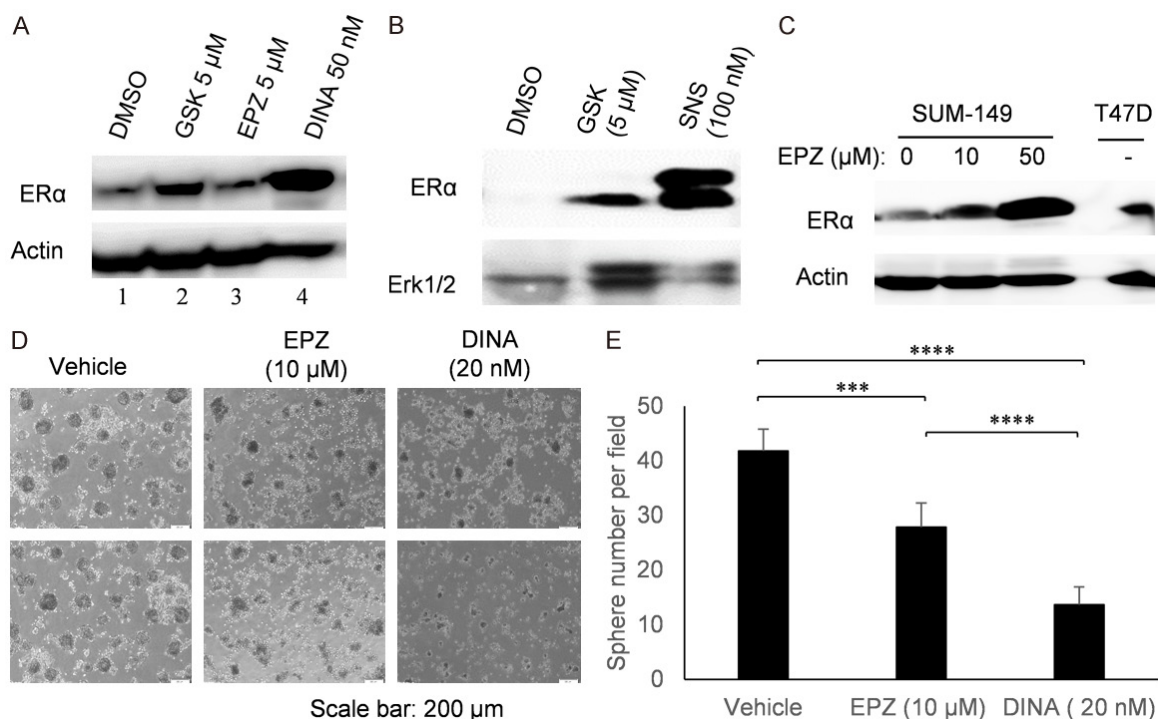


Figure 4. A comparison of the inhibitory effects between EZH2i and CDK2i on ER α induction and tumor sphere formation. TNBC cell line MDA-MB-231 cells were treated with 50 nM dinaciclib (DINA) and 5 μ M EPZ-6438 (EPZ) and GSK343 (GSK) for 72 hours. ER α protein levels in the inhibitor-treated cell lysates were detected by an immunoblotting analysis with specific antibodies against ER α . Actin was used as the loading control. (B) MDA-MB-231 cells were treated with 5 μ M GSK343 (GSK) and 100 nM CDK2i SNS032 (SNS) as described in (A). (C). EZH2i-induced ER α expression in TNBCs was dose-dependent. TNBC cell line SUM-149 cells were treated with EPZ-6438 (EPZ) at different concentration for 72 hours. ER α protein levels were immunoblotted as described in (A), and T47D cell lysate was used for ER α -positive control. (D, E) The inhibitory effects of CDK2i and EZH2i on tumor sphere formation. MDA-MB-231 (5,000) cells in 2.5% Matrigel were seeded in Matrigel-coated 24-well plate and incubated at 37 $^{\circ}$ C for 3 days followed by treatment with CDK2 and EZH2 inhibitors for 1 week. Representative images (D) and quantitation (E) of the spheres are shown. ***, $P < 0.001$; ****, $P < 0.0001$, Student's t-test. Scale bar, 200 μ m.

results were observed in the HGSOC cell line SKOV3 after treatment with EZH2i (**Figure 5C**). These findings indicated that inhibition of EZH2 activity in the CDK2-EZH2 axis by the specific EZH2i led to a feedback CDK2 activation as indicated by increased pCDK2(T160), and this in turn compromises the inhibitory effects of EZH2i in the breast and ovarian cancer cells (**Figure 5B** and **5C**). These findings revealed a new potential connection: incomplete inhibition of EZH2 activity could upregulate CDK2 phosphorylation via a feedback loop, which in turn increases EZH2 phosphorylation and thus undermines the effects of EZH2i (**Figure 5D**). Taken together, our findings suggested that the compromised inhibitory effects of EZH2i in cancer cells is partly attributed to a feedback loop of the CDK2-EZH2 signaling axis. Therefore, to achieve complete inhibition of

EZH2 activity, a persistent higher dose of EZH2i is required.

Discussion

Our data demonstrated that similar to TNBC, blockade of the CDK2/EZH2 axis by CDK2i or EZH2i reactivated ER α expression in HGSOCs, rendering the cancer cells sensitive to hormonal therapy. In addition, partial inhibition of EZH2 activity by EZH2i compromised the inhibitory effects of EZH2i on both of TNBC and HGSOC via a feedback mechanism.

EZH2 activity is regulated by phosphorylation/dephosphorylation, leading to alternation in trimethylation of H3K27 and subsequently epigenetic silencing or de-repressing of the target genes [2, 3, 5, 6, 36]. Accumulating evidence demonstrates that EZH2 is aberrantly overex-

CDK2 inhibitor inhibits phosphorylation of EZH2 to activate ER α expression

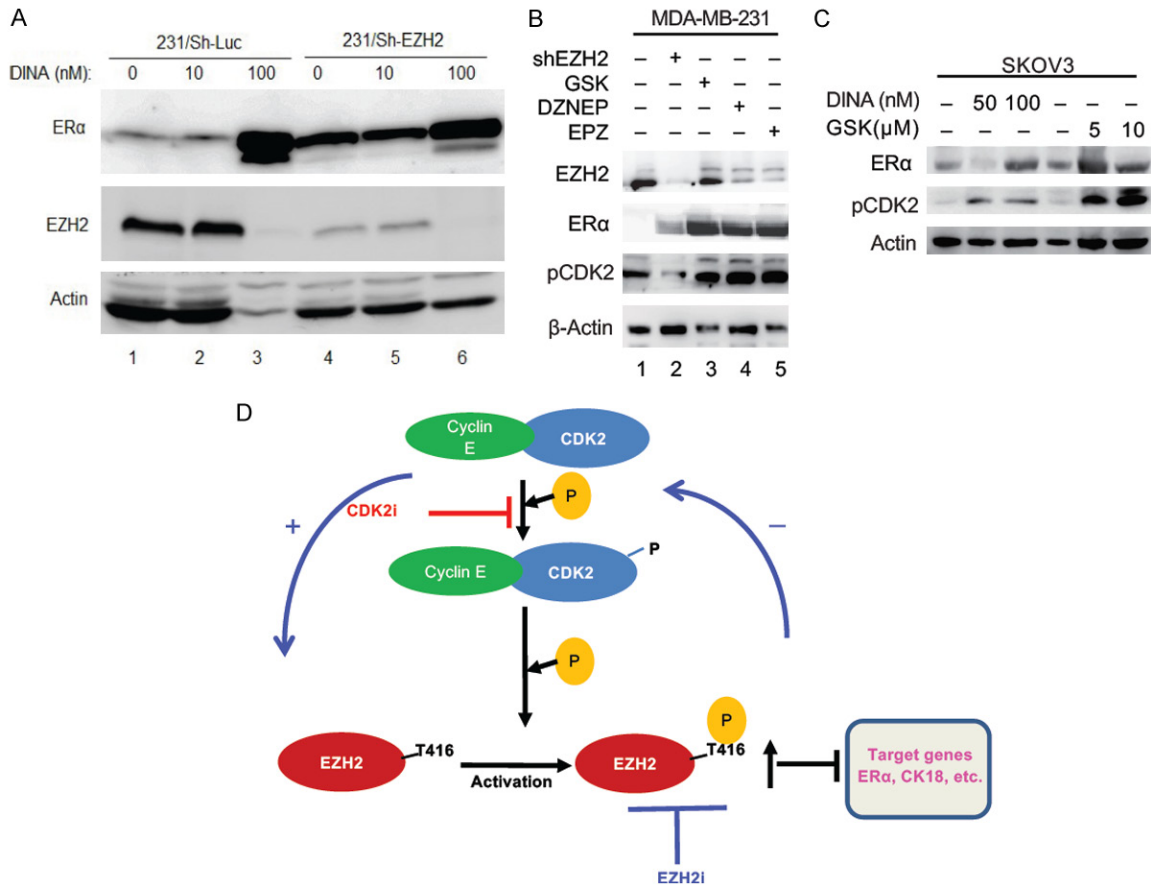


Figure 5. EZH2i enhances CDK2 activity by feedback loop in breast and ovarian cancer cells. (A) MDA-MB-231 control cells (sh-Luc) and EZH2-Knockdown cells (sh-EZH2) were treated with different doses of dinaciclib (DINA) for 72 hours. ER α and EZH2 proteins in the whole cell lysates were separated on 10% SDS- polyacrylamide gel and immunoblotted with indicated specific antibodies. (B) MDA-MB-231 control and sh-EZH2 cells were treated with 5 μ M GSK343 (GSK), 5 μ M 3-deazaneplanocin A hydrochloride (DZNEP) and 20 μ M EPZ-6438 (EPZ) for 3 days. Immunoblotting analysis of the treated cells were performed with indicated specific antibodies. (C) SKOV3 cells were treated with different doses of DINA or GSK and analyzed as described in (A). (D) A model illustrating the CDK2-EZH2 axis feedback loop. CDK2-mediated phosphorylation of EZH2 at T416 activates EZH2 to silence target genes, and higher EZH2 activity triggers a negative feedback inhibition of CDK2 activation to maintain homeostasis of the signaling axis. CDK2i and EZH2i block the CDK2-EZH2 signaling axis and thus repress the EZH2 target genes. Incomplete inhibition of EZH2 results in feedback activation of CDK2, compromising EZH2i efficacy.

pressed in different types of solid tumors and is associated with metastasis and progression [39, 40]. We previously reported that phospho-EZH2 binds to the promoter of ER α to repress the expression of ER α in TNBC and that blocking phosphorylation of EZH2 at T416 with CDK2i reactivates ER α expression, thereby rendering cancer cells targetable by tamoxifen in TNBC [30]. In the current study, we observed that similar to TNBC, blockade of the CDK2/EZH2 axis in ER α -negative HGSOC cell lines with specific inhibitors led to the induction of ER α expression, rendering HGSOC targetable by hormone therapy. It has been reported that

about 81% of HGSOC express ER α [11]. The rationale for endocrine maintenance therapy for HGSOC, which is partially driven by the estrogen pathway, is based on high ER α expression. The expression levels of ER α are correlated with endocrine sensitivity in HGSOC [26]. Hormone therapy for patients with HGSOC results in a significant benefit, particularly in those with relapsed, ER positive diseases [31]. The development of an approach to convert ER α -negative to positive in HGSOC provides an alternative choice of combination treatment for those patients, and thus has important clinical significance. Our observations in vitro revealed

CDK2 inhibitor inhibits phosphorylation of EZH2 to activate ER α expression

that ER α and its downstream target genes were re-activated in response to CDK2/EZH2 axis blockade with specific inhibitors in ovarian cancer cell lines SKOV3, OVCA433, and CAOV3. However, the CDK2i-treated ovarian cancer cell lines DOV13 and A2780 failed to reactivate ER α expression (**Figure 2A**). The underlying mechanism of this failure remains to be further investigated.

Our findings indicated that the magnitude of the CDK2i and EZH2i-induced inhibitory effects on tumor growth in vitro and in vivo was significantly different (e.g., 25-100 nM dinaciclib vs. 2.5 μ M EPZ-6438 or 5 μ M GSK343) (**Figure 4**). CDK2i was much more efficient than EZH2i at the doses tested (**Figure 4**) [19, 30, 38]. It has been reported that CDKs have a critical role in cell cycle progression and that they govern a large number of targets for novel anticancer drug development [41, 42]. A previous study demonstrated that CDK2i represses the phosphorylation of EZH2 and inhibits tumor cell growth [43]. To identify the underlying mechanism of the difference in efficacy between CDK2i and EZH2i in the cancer cells, we examined the CDK2 activity in the EZH2i-treated TNBC and HGSOC cells. An increase of phospho-CDK2 at T160 (pCDK2) suggested that inhibition of EZH2 activity triggered an upregulation of CDK2 phosphorylation, which in turn increased EZH2 activation (**Figure 5D**). This homeostatic mechanism maintains the activation of EZH2 in the loop and impairs the efficiency of EZH2i. The phenomenon also implies that full blockade of the CDK2-EZH2 axis by targeting EZH2 requires a high dose of EZH2i (**Figure 5D**). Indeed, previous in vivo studies demonstrated more than 300 mg/kg of EPZ-6438 and 2-8 mg/kg of dinaciclib had the same potency in inhibiting tumor growth [30, 38, 44]. The putative homeostatic feedback loop might at least partly explain the insensitivity of tumors to EZH2i compared with CDK2i. However, the underlying mechanism of feedback regulation on the CDK2-EZH2 signaling pathway remains to be further investigated. According to our results and those from previous reports, CDK2i not only directly inhibits cell cycle but also inactivates the oncogenic EZH2 activity, leading to the release of epigenetic repression in target genes [6, 18, 30]. Moreover, CDK2i more potently blocked the CDK2/EZH2 axis than did EZH2i in inhibiting phosphorylation of EZH2 and in exerting a cytotoxic effect

on tumor cells without feedback up-regulation of EZH2 activity (**Figure 5D**).

In summary, this study provides additional evidence that ER α expression can be induced in HGSOC and TNBC treated with CDK2i and EZH2i. The combination therapy with CDK2i and tamoxifen demonstrated a synergistic inhibitory effect on the HGSOC cell proliferation and may be an alternative treatment approach for HGSOC patients with ER α -negative disease. Further in vivo studies are needed before it can be evaluated in clinical trials.

Acknowledgements

This work was funded in part by the following: National Institutes of Health (CCSG CA016672); Cancer Prevention & Research Institutes of Texas (RP160710); National Breast Cancer Foundation, Inc.; Patel Memorial Breast Cancer Endowment Fund; Breast Cancer Research Foundation; The University of Texas MD Anderson-China Medical University and Hospital Sister Institution Fund (to M.-C.H.) and Taiwan's New Partnership Program For The Connection To The Top Labs In The World (Dragon Gate Program; 107-2911-I-006-519; to Y.-Y.C.); We thank Ann M. Sutton, Scientific Publications Research Medical Library, The University of Texas MD Anderson Cancer Center for critically reading and editing this manuscript.

Disclosure of conflict of interest

None.

Address correspondence to: Mien-Chie Hung, Office of The President, China Medical University, Taichung 404, Taiwan. E-mail: mhung@cmu.edu.tw; Lei Nie, Department of Molecular and Cellular Oncology, Unit 108, The University of Texas MD Anderson Cancer Center, Houston, TX 77030, USA. E-mail: lnjie@mdanderson.org

References

- [1] Kim KH and Roberts CW. Targeting EZH2 in cancer. *Nat Med* 2016; 22: 128-134.
- [2] Chang CJ and Hung MC. The role of EZH2 in tumour progression. *Br J Cancer* 2012; 106: 243-247.
- [3] Yamaguchi H and Hung MC. Regulation and role of EZH2 in cancer. *Cancer Res Treat* 2014; 46: 209-222.

CDK2 inhibitor inhibits phosphorylation of EZH2 to activate ER α expression

- [4] Laugesen A, Højfeldt JW and Helin K. Molecular mechanisms directing PRC2 recruitment and H3K27 methylation. *Mol Cell* 2019; 74: 8-18.
- [5] Wei Y, Chen YH, Li LY, Lang J, Yeh SP, Shi B, Yang CC, Yang JY, Lin CY, Lai CC and Hung MC. CDK1-dependent phosphorylation of EZH2 suppresses methylation of H3K27 and promotes osteogenic differentiation of human mesenchymal stem cells. *Nat Cell Biol* 2011; 13: 87-94.
- [6] Yang CC, LaBaff A, Wei Y, Nie L, Xia W, Huo L, Yamaguchi H, Hsu YH, Hsu JL, Liu D, Lang J, Du Y, Lien HC, Li LY, Deng R, Chan LC, Yao J, Klee CG, Hortobagyi GN and Hung MC. Phosphorylation of EZH2 at T416 by CDK2 contributes to the malignancy of triple negative breast cancers. *Am J Transl Res* 2015; 7: 1009-1020.
- [7] Chang CJ, Yang JY, Xia W, Chen CT, Xie X, Chao CH, Woodward WA, Hsu JM, Hortobagyi GN and Hung MC. EZH2 promotes expansion of breast tumor initiating cells through activation of RAF1-beta-catenin signaling. *Cancer Cell* 2011; 19: 86-100.
- [8] De Brot M, Rocha RM, Soares FA and Gobbi H. Prognostic impact of the cancer stem cell related markers ALDH1 and EZH2 in triple negative and basal-like breast cancers. *Pathology* 2012; 44: 303-312.
- [9] Huang X, Yan J, Zhang M, Wang Y, Chen Y, Fu X, Wei R, Zheng XL, Liu Z, Zhang X, Yang H, Hao B, Shen YY, Su Y, Cong X, Huang M, Tan M, Ding J and Geng M. Targeting epigenetic crosstalk as a therapeutic strategy for EZH2-aberrant solid tumors. *Cell* 2018; 175: 186-199, e119.
- [10] Jones BA, Varambally S and Arend RC. Histone methyltransferase EZH2: a therapeutic target for ovarian cancer. *Mol Cancer Ther* 2018; 17: 591-602.
- [11] Sieh W, Kobel M, Longacre TA, Bowtell DD, deFazio A, Goodman MT, Hogdall E, Deen S, Wentzensen N, Moysich KB, Brenton JD, Clarke BA, Menon U, Gilks CB, Kim A, Madore J, Fereday S, George J, Galletta L, Lurie G, Wilkens LR, Carney ME, Thompson PJ, Matsuno RK, Kjaer SK, Jensen A, Hogdall C, Kalli KR, Fridley BL, Keeney GL, Vierkant RA, Cunningham JM, Brinton LA, Yang HP, Sherman ME, Garcia-Closas M, Lissowska J, Odunsi K, Morrison C, Lele S, Bshara W, Sucheston L, Jimenez-Linan M, Driver K, Alsop J, Mack M, McGuire V, Rothstein JH, Rosen BP, Bernardini MQ, Mackay H, Oza A, Wozniak EL, Benjamin E, Gentry-Maharaj A, Gayther SA, Tinker AV, Prentice LM, Chow C, Anglesio MS, Johnatty SE, Chenevix-Trench G, Whittemore AS, Pharoah PD, Goode EL, Huntsman DG and Ramus SJ. Hormone-receptor expression and ovarian cancer survival: an ovarian tumor tissue analysis consortium study. *Lancet Oncol* 2013; 14: 853-862.
- [12] Siegel RL, Miller KD and Jemal A. Cancer statistics, 2019. *CA Cancer J Clin* 2019; 69: 7-34.
- [13] Reid BM, Permuth JB and Sellers TA. Epidemiology of ovarian cancer: a review. *Cancer Biol Med* 2017; 14: 9-32.
- [14] Siegel RL, Miller KD and Jemal A. Cancer statistics, 2018. *CA Cancer J Clin* 2018; 68: 7-30.
- [15] Kroeger PT Jr and Drapkin R. Pathogenesis and heterogeneity of ovarian cancer. *Curr Opin Obstet Gynecol* 2017; 29: 26-34.
- [16] Lisio MA, Fu L, Goyeneche A, Gao ZH and Telleria C. High-grade serous ovarian cancer: basic sciences, clinical and therapeutic standpoints. *Int J Mol Sci* 2019; 20.
- [17] Au-Yeung G, Lang F, Azar WJ, Mitchell C, Jarman KE, Lackovic K, Aziz D, Cullinane C, Pearson RB, Mileskin L, Rischin D, Karst AM, Drapkin R, Etemadmoghadam D and Bowtell DD. Selective targeting of cyclin E1-amplified high-grade serous ovarian cancer by cyclin-dependent kinase 2 and AKT inhibition. *Clin Cancer Res* 2017; 23: 1862-1874.
- [18] Fang D, Huang S and Su SB. Cyclin E1-CDK 2, a potential anticancer target. *Aging (Albany NY)* 2016; 8: 571-572.
- [19] Kumar SK, LaPlant B, Chng WJ, Zonder J, Callander N, Fonseca R, Fruth B, Roy V, Erlichman C, Stewart AK and Mayo Phase C. Dinaciclib, a novel CDK inhibitor, demonstrates encouraging single-agent activity in patients with relapsed multiple myeloma. *Blood* 2015; 125: 443-448.
- [20] Mita MM, Joy AA, Mita A, Sankhala K, Jou YM, Zhang D, Statkevich P, Zhu Y, Yao SL, Small K, Bannerji R and Shapiro CL. Randomized phase II trial of the cyclin-dependent kinase inhibitor dinaciclib (MK-7965) versus capecitabine in patients with advanced breast cancer. *Clin Breast Cancer* 2014; 14: 169-176.
- [21] Mita MM, Mita AC, Moseley JL, Poon J, Small KA, Jou YM, Kirschmeier P, Zhang D, Zhu Y, Statkevich P, Sankhala KK, Sarantopoulos J, Cleary JM, Chirieac LR, Rodig SJ, Bannerji R and Shapiro GI. Phase 1 safety, pharmacokinetic and pharmacodynamic study of the cyclin-dependent kinase inhibitor dinaciclib administered every three weeks in patients with advanced malignancies. *Br J Cancer* 2017; 117: 1258-1268.
- [22] Hogdall EV, Christensen L, Hogdall CK, Blaakaer J, Gayther S, Jacobs IJ, Christensen IJ and Kjaer SK. Prognostic value of estrogen receptor and progesterone receptor tumor expression in Danish ovarian cancer patients: from the 'MALOVA' ovarian cancer study. *Oncol Rep* 2007; 18: 1051-1059.

CDK2 inhibitor inhibits phosphorylation of EZH2 to activate ER α expression

- [23] Halon A, Nowak-Markwitz E, Maciejczyk A, Pudelko M, Gansukh T, Gyorffy B, Donizy P, Murawa D, Matkowski R, Spaczynski M, Lage H and Surowiak P. Loss of estrogen receptor beta expression correlates with shorter overall survival and lack of clinical response to chemotherapy in ovarian cancer patients. *Anticancer Res* 2011; 31: 711-718.
- [24] Yaşar P, Ayaz G, User SD, Güpür G and Muyan M. Molecular mechanism of estrogen-estrogen receptor signaling. *Reprod Med Biol* 2016; 16: 4-20.
- [25] Simpkins F, Hevia-Paez P, Sun J, Ullmer W, Gilbert CA, da Silva T, Pedram A, Levin ER, Reis IM, Rabinovich B, Azzam D, Xu XX, Ince TA, Yang JY, Verhaak RG, Lu Y, Mills GB and Slingerland JM. Src Inhibition with saracatinib reverses fulvestrant resistance in ER-positive ovarian cancer models in vitro and in vivo. *Clin Cancer Res* 2012; 18: 5911-5923.
- [26] Stanley B, Hollis RL, Nunes H, Towler JD, Yan X, Rye T, Dawson C, Mackean MJ, Nussey F, Churchman M, Herrington CS and Gourley C. Endocrine treatment of high grade serous ovarian carcinoma; quantification of efficacy and identification of response predictors. *Gynecol Oncol* 2019; 152: 278-285.
- [27] Andersen CL, Sikora MJ, Boisen MM, Ma T, Christie A, Tseng G, Park Y, Luthra S, Chandran U, Haluska P, Mantia-Saldone GM, Odunsi K, McLean K, Lee AV, Elishaev E, Edwards RP and Oesterreich S. Active estrogen receptor-alpha signaling in ovarian cancer models and clinical specimens. *Clin Cancer Res* 2017; 23: 3802-3812.
- [28] Tseng OL, Spinelli JJ, Gotay CC, Ho WY, McBride ML and Dawes MG. Aromatase inhibitors are associated with a higher fracture risk than tamoxifen: a systematic review and meta-analysis. *Ther Adv Musculoskelet Dis* 2018; 10: 71-90.
- [29] Fleming CA, Heneghan HM, O'Brien D, McCartan DP, McDermott EW and Prichard RS. Meta-analysis of the cumulative risk of endometrial malignancy and systematic review of endometrial surveillance in extended tamoxifen therapy. *Br J Surg* 2018; 105: 1098-1106.
- [30] Nie L, Wei Y, Zhang F, Hsu YH, Chan LC, Xia W, Ke B, Zhu C, Deng R, Tang J, Yao J, Chu YY, Zhao X, Han Y, Hou J, Huo L, Ko HW, Lin WC, Yamaguchi H, Hsu JM, Yang Y, Pan DN, Hsu JL, Kleer CG, Davidson NE, Hortobagyi GN and Hung MC. CDK2-mediated site-specific phosphorylation of EZH2 drives and maintains triple-negative breast cancer. *Nat Commun* 2019; 10: 5114.
- [31] Stanley B, Hollis RL, Nunes H, Towler JD, Yan X, Rye T, Dawson C, Mackean MJ, Nussey F, Churchman M, Herrington CS and Gourley C. Endocrine treatment of high grade serous ovarian carcinoma; quantification of efficacy and identification of response predictors. *Gynecol Oncol* 2019; 152: 278-285.
- [32] Yoshihara K, Tajima A, Komata D, Yamamoto T, Kodama S, Fujiwara H, Suzuki M, Onishi Y, Hatae M, Sueyoshi K, Fujiwara H, Kudo Y, Inoue I and Tanaka K. Gene expression profiling of advanced-stage serous ovarian cancers distinguishes novel subclasses and implicates ZEB2 in tumor progression and prognosis. *Cancer Sci* 2009; 100: 1421-1428.
- [33] Chou TC. Drug combination studies and their synergy quantification using the Chou-Talalay method. *Cancer Res* 2010; 70: 440-446.
- [34] Chou TC. Theoretical basis, experimental design, and computerized simulation of synergism and antagonism in drug combination studies. *Pharmacol Rev* 2006; 58: 621-681.
- [35] Minnebo N, Gornemann J, O'Connell N, Van Dessel N, Derua R, Vermunt MW, Page R, Beullens M, Peti W, Van Eynde A and Bollen M. NIPP1 maintains EZH2 phosphorylation and promoter occupancy at proliferation-related target genes. *Nucleic Acids Res* 2013; 41: 842-854.
- [36] Chen S, Bohrer LR, Rai AN, Pan Y, Gan L, Zhou X, Bagchi A, Simon JA and Huang H. Cyclin-dependent kinases regulate epigenetic gene silencing through phosphorylation of EZH2. *Nat Cell Biol* 2010; 12: 1108-1114.
- [37] Kaneko S, Li G, Son J, Xu CF, Margueron R, Neubert TA and Reinberg D. Phosphorylation of the PRC2 component Ezh2 is cell cycle-regulated and up-regulates its binding to ncRNA. *Genes Dev* 2010; 24: 2615-2620.
- [38] Knutson SK, Kawano S, Minoshima Y, Warholik NM, Huang KC, Xiao Y, Kadowaki T, Uesugi M, Kuznetsov G, Kumar N, Wigle TJ, Klaus CR, Allain CJ, Raimondi A, Waters NJ, Smith JJ, Porter-Scott M, Chesworth R, Moyer MP, Copeland RA, Richon VM, Uenaka T, Pollock RM, Kuntz KW, Yokoi A and Keilhack H. Selective inhibition of EZH2 by EPZ-6438 leads to potent anti-tumor activity in EZH2-mutant non-Hodgkin lymphoma. *Mol Cancer Ther* 2014; 13: 842-854.
- [39] Nienstedt JC, Schroeder C, Clauditz T, Simon R, Sauter G, Muenscher A, Blessmann M, Hanken H and Pflug C. EZH2 overexpression in head and neck cancer is related to lymph node metastasis. *J Oral Pathol Med* 2018; 47: 240-245.
- [40] Liu Y, Yu K, Li M, Zeng K, Wei J, Li X, Liu Y, Zhao D, Fan L, Yu Z, Wang Y, Li Z, Zhang W, Bai Q, Yan Q, Guo Y, Wang Z and Guo S. EZH2 overexpression in primary gastrointestinal diffuse large B-cell lymphoma and its association with

CDK2 inhibitor inhibits phosphorylation of EZH2 to activate ER α expression

- the clinicopathological features. *Hum Pathol* 2017; 64: 213-221.
- [41] Yang B, Jia Y, Jia Z, Wang W, Song X, Li Y, Yi Q, Wang L and Song L. The cyclin-dependent kinase 2 (CDK2) mediates hematopoiesis through G1-to-S transition in Chinese mitten crab *Eriocheir sinensis*. *Dev Comp Immunol* 2018; 81: 156-166.
- [42] Whittaker SR, Barlow C, Martin MP, Mancusi C, Wagner S, Self A, Barrie E, Te Poele R, Sharp S, Brown N, Wilson S, Jackson W, Fischer PM, Clarke PA, Walton MI, McDonald E, Blagg J, Noble M, Garrett MD and Workman P. Molecular profiling and combinatorial activity of CCT068127: a potent CDK2 and CDK9 inhibitor. *Mol Oncol* 2018; 12: 287-304.
- [43] Volkart PA, Bitencourt-Ferreira G, Souto AA and de Azevedo WF. Cyclin-dependent kinase 2 in cellular senescence and cancer. A structural and functional review. *Curr Drug Targets* 2019; 20: 716-726.
- [44] Johnson SF, Cruz C, Greifenberg AK, Dust S, Stover DG, Chi D, Primack B, Cao S, Bernhardt AJ, Coulson R, Lazaro JB, Kochupurakkal B, Sun H, Unitt C, Moreau LA, Sarosiek KA, Scaltriti M, Juric D, Baselga J, Richardson AL, Rodig SJ, D'Andrea AD, Balmana J, Johnson N, Geyer M, Serra V, Lim E and Shapiro GI. CDK12 inhibition reverses de novo and acquired PARP inhibitor resistance in BRCA wild-type and mutated models of triple-negative breast cancer. *Cell Rep* 2016; 17: 2367-2381.

CDK2 inhibitor inhibits phosphorylation of EZH2 to activate ER α expression

Table S1. Yoshihara Ovarian

Sample Number	Sample Name	Cancer and Normal Type	Cancer Sample Site	Cancer Type	GEO ID	Normal Tissue Type	Sample Type	Sex	Stage	Gene/Reporter	EZH2/A_23_P259641
1	Peritoneum normal 3	Peritoneum			GSM311992	Peritoneum	Surgical Specimen	Female			0.67156
2	Peritoneum normal 4	Peritoneum			GSM312129	Peritoneum	Surgical Specimen	Female			1.44516
3	Peritoneum normal 7	Peritoneum			GSM312130	Peritoneum	Surgical Specimen	Female			1.50723
4	Peritoneum normal 12	Peritoneum			GSM312131	Peritoneum	Surgical Specimen	Female			2.44561
5	Peritoneum normal 15	Peritoneum			GSM312132	Peritoneum	Surgical Specimen	Female			1.152
6	Peritoneum normal 16	Peritoneum			GSM312133	Peritoneum	Surgical Specimen	Female			0.66181
7	Peritoneum normal 18	Peritoneum			GSM312134	Peritoneum	Surgical Specimen	Female			1.67876
8	Peritoneum normal 21	Peritoneum			GSM312135	Peritoneum	Surgical Specimen	Female			-0.7241
9	Peritoneum normal 23	Peritoneum			GSM312136	Peritoneum	Surgical Specimen	Female			0.48063
10	Peritoneum normal 30	Peritoneum			GSM312137	Peritoneum	Surgical Specimen	Female			0.53766
11	Advanced serous ovarian cancer 2	Ovarian Serous Adenocarcinoma	Primary Site	Ovarian Serous Adenocarcinoma	GSM312138		Surgical Specimen	Female	Stage III or IV		3.22924
12	Advanced serous ovarian cancer 6	Ovarian Serous Adenocarcinoma	Primary Site	Ovarian Serous Adenocarcinoma	GSM312139		Surgical Specimen	Female	Stage III or IV		4.95661
13	Advanced serous ovarian cancer 7	Ovarian Serous Adenocarcinoma	Primary Site	Ovarian Serous Adenocarcinoma	GSM312140		Surgical Specimen	Female	Stage III or IV		3.17089
14	Advanced serous ovarian cancer 11	Ovarian Serous Adenocarcinoma	Primary Site	Ovarian Serous Adenocarcinoma	GSM312141		Surgical Specimen	Female	Stage III or IV		3.84012
15	Advanced serous ovarian cancer 17	Ovarian Serous Adenocarcinoma	Primary Site	Ovarian Serous Adenocarcinoma	GSM312142		Surgical Specimen	Female	Stage III or IV		2.51785
16	Advanced serous ovarian cancer 18	Ovarian Serous Adenocarcinoma	Primary Site	Ovarian Serous Adenocarcinoma	GSM312143		Surgical Specimen	Female	Stage III or IV		4.08637
17	Advanced serous ovarian cancer 20	Ovarian Serous Adenocarcinoma	Primary Site	Ovarian Serous Adenocarcinoma	GSM312144		Surgical Specimen	Female	Stage III or IV		4.59018
18	Advanced serous ovarian cancer 24	Ovarian Serous Adenocarcinoma	Primary Site	Ovarian Serous Adenocarcinoma	GSM312145		Surgical Specimen	Female	Stage III or IV		4.99214
19	Advanced serous ovarian cancer 25	Ovarian Serous Adenocarcinoma	Primary Site	Ovarian Serous Adenocarcinoma	GSM312146		Surgical Specimen	Female	Stage III or IV		5.21594
20	Advanced serous ovarian cancer 36	Ovarian Serous Adenocarcinoma	Primary Site	Ovarian Serous Adenocarcinoma	GSM312147		Surgical Specimen	Female	Stage III or IV		3.59877
21	Advanced serous ovarian cancer 37	Ovarian Serous Adenocarcinoma	Primary Site	Ovarian Serous Adenocarcinoma	GSM312148		Surgical Specimen	Female	Stage III or IV		3.04826
22	Advanced serous ovarian cancer 38	Ovarian Serous Adenocarcinoma	Primary Site	Ovarian Serous Adenocarcinoma	GSM312149		Surgical Specimen	Female	Stage III or IV		3.26437
23	Advanced serous ovarian cancer 43	Ovarian Serous Adenocarcinoma	Primary Site	Ovarian Serous Adenocarcinoma	GSM312150		Surgical Specimen	Female	Stage III or IV		2.37895
24	Advanced serous ovarian cancer 49	Ovarian Serous Adenocarcinoma	Primary Site	Ovarian Serous Adenocarcinoma	GSM312151		Surgical Specimen	Female	Stage III or IV		3.46566
25	Advanced serous ovarian cancer 54	Ovarian Serous Adenocarcinoma	Primary Site	Ovarian Serous Adenocarcinoma	GSM312152		Surgical Specimen	Female	Stage III or IV		3.67726

CDK2 inhibitor inhibits phosphorylation of EZH2 to activate ER α expression

26	Advanced serous ovarian cancer 57	Ovarian Serous Adenocarcinoma	Primary Site	Ovarian Serous Adenocarcinoma	GSM312153	Surgical Specimen	Female	Stage III or IV	3.08453
27	Advanced serous ovarian cancer 61	Ovarian Serous Adenocarcinoma	Primary Site	Ovarian Serous Adenocarcinoma	GSM312154	Surgical Specimen	Female	Stage III or IV	4.28478
28	Advanced serous ovarian cancer 10	Ovarian Serous Adenocarcinoma	Primary Site	Ovarian Serous Adenocarcinoma	GSM312155	Surgical Specimen	Female	Stage III or IV	3.43929
29	Advanced serous ovarian cancer 15	Ovarian Serous Adenocarcinoma	Primary Site	Ovarian Serous Adenocarcinoma	GSM312156	Surgical Specimen	Female	Stage III or IV	3.76306
30	Advanced serous ovarian cancer 23	Ovarian Serous Adenocarcinoma	Primary Site	Ovarian Serous Adenocarcinoma	GSM312157	Surgical Specimen	Female	Stage III or IV	1.74904
31	Advanced serous ovarian cancer 27	Ovarian Serous Adenocarcinoma	Primary Site	Ovarian Serous Adenocarcinoma	GSM312158	Surgical Specimen	Female	Stage III or IV	4.18027
32	Advanced serous ovarian cancer 39	Ovarian Serous Adenocarcinoma	Primary Site	Ovarian Serous Adenocarcinoma	GSM312159	Surgical Specimen	Female	Stage III or IV	3.32193
33	Advanced serous ovarian cancer 42	Ovarian Serous Adenocarcinoma	Primary Site	Ovarian Serous Adenocarcinoma	GSM312160	Surgical Specimen	Female	Stage III or IV	3.74819
34	Advanced serous ovarian cancer 45	Ovarian Serous Adenocarcinoma	Primary Site	Ovarian Serous Adenocarcinoma	GSM312161	Surgical Specimen	Female	Stage III or IV	4.05261
35	Advanced serous ovarian cancer 46	Ovarian Serous Adenocarcinoma	Primary Site	Ovarian Serous Adenocarcinoma	GSM312162	Surgical Specimen	Female	Stage III or IV	1.06123
36	Advanced serous ovarian cancer 50	Ovarian Serous Adenocarcinoma	Primary Site	Ovarian Serous Adenocarcinoma	GSM312163	Surgical Specimen	Female	Stage III or IV	3.92157
37	Advanced serous ovarian cancer 51	Ovarian Serous Adenocarcinoma	Primary Site	Ovarian Serous Adenocarcinoma	GSM312165	Surgical Specimen	Female	Stage III or IV	3.49613
38	Advanced serous ovarian cancer 52	Ovarian Serous Adenocarcinoma	Primary Site	Ovarian Serous Adenocarcinoma	GSM312167	Surgical Specimen	Female	Stage III or IV	3.04351
39	Advanced serous ovarian cancer 53	Ovarian Serous Adenocarcinoma	Primary Site	Ovarian Serous Adenocarcinoma	GSM312168	Surgical Specimen	Female	Stage III or IV	4.118
40	Advanced serous ovarian cancer 55	Ovarian Serous Adenocarcinoma	Primary Site	Ovarian Serous Adenocarcinoma	GSM312170	Surgical Specimen	Female	Stage III or IV	2.4133
41	Advanced serous ovarian cancer 56	Ovarian Serous Adenocarcinoma	Primary Site	Ovarian Serous Adenocarcinoma	GSM312171	Surgical Specimen	Female	Stage III or IV	3.19819
42	Advanced serous ovarian cancer 58	Ovarian Serous Adenocarcinoma	Primary Site	Ovarian Serous Adenocarcinoma	GSM312172	Surgical Specimen	Female	Stage III or IV	3.96941
43	Advanced serous ovarian cancer 60	Ovarian Serous Adenocarcinoma	Primary Site	Ovarian Serous Adenocarcinoma	GSM312173	Surgical Specimen	Female	Stage III or IV	2.08342
44	Advanced serous ovarian cancer 62	Ovarian Serous Adenocarcinoma	Primary Site	Ovarian Serous Adenocarcinoma	GSM312174	Surgical Specimen	Female	Stage III or IV	2.71546
45	Advanced serous ovarian cancer 64	Ovarian Serous Adenocarcinoma	Primary Site	Ovarian Serous Adenocarcinoma	GSM312175	Surgical Specimen	Female	Stage III or IV	3.53605
46	Early serous ovarian cancer 5	Ovarian Serous Adenocarcinoma	Primary Site	Ovarian Serous Adenocarcinoma	GSM312176	Surgical Specimen	Female	Stage I	4.50779
47	Early serous ovarian cancer 8	Ovarian Serous Adenocarcinoma	Primary Site	Ovarian Serous Adenocarcinoma	GSM312178	Surgical Specimen	Female	Stage I	3.47874
48	Early serous ovarian cancer 9	Ovarian Serous Adenocarcinoma	Primary Site	Ovarian Serous Adenocarcinoma	GSM312179	Surgical Specimen	Female	Stage I	3.9775

CDK2 inhibitor inhibits phosphorylation of EZH2 to activate ER α expression

49	Early serous ovarian cancer 28	Ovarian Serous Adenocarcinoma	Primary Site	Ovarian Serous Adenocarcinoma	GSM312180	Surgical Specimen	Female	Stage I	5.83062
50	Early serous ovarian cancer 32	Ovarian Serous Adenocarcinoma	Primary Site	Ovarian Serous Adenocarcinoma	GSM312181	Surgical Specimen	Female	Stage I	3.06128
51	Early serous ovarian cancer 33	Ovarian Serous Adenocarcinoma	Primary Site	Ovarian Serous Adenocarcinoma	GSM312182	Surgical Specimen	Female	Stage I	3.90004
52	Early serous ovarian cancer 35	Ovarian Serous Adenocarcinoma	Primary Site	Ovarian Serous Adenocarcinoma	GSM312183	Surgical Specimen	Female	Stage I	3.15669
53	Early serous ovarian cancer 65	Ovarian Serous Adenocarcinoma	Primary Site	Ovarian Serous Adenocarcinoma	GSM312185	Surgical Specimen	Female	Stage I	3.02495